

Article

Ammonia Sensing Behaviors of TiO₂-PANI/PA6 Composite Nanofibers

Qingqing Wang, Xianjun Dong, Zengyuan Pang, Yuanzhi Du, Xin Xia, Qifu Wei * and Fenglin Huang

Key Laboratory of Eco-Textiles, Ministry of Education, Jiangnan University, Wuxi 214122, Jiangsu, China; E-Mails: wqq888217@126.com (Q.W.); crivia1988@hotmail.com (X.D.); pangzengyuan1212@163.com (Z.P.); dyzddd@163.com (Y.D.); xjxiaxin@163.com (X.X.); windhuang325@163.com (F.H.)

* Author to whom correspondence should be addressed; E-Mail: qfwei@jiangnan.edu.cn; Tel.: +86-510-8591-3653; Fax: +86-510-8591-2009.

Received: 26 October 2012; in revised form: 27 November 2012 / Accepted: 3 December 2012 / Published: 12 December 2012

Abstract: Titanium dioxide-polyaniline/polyamide 6 (TiO₂-PANI/PA6) composite nanofibers were prepared by *in situ* polymerization of aniline in the presence of PA6 nanofibers and a sputtering-deposition process with a high purity titanium sputtering target. TiO₂-PANI/PA6 composite nanofibers and PANI/PA6 composite nanofibers were fabricated for ammonia gas sensing. The ammonia sensing behaviors of the sensors were examined at room temperature. All the results indicated that the ammonia sensing property of TiO₂-PANI/PA6 composite nanofibers was superior to that of PANI/PA6 composite nanofibers. TiO₂-PANI/PA6 composite nanofibers had good selectivity to ammonia. It was also found that the content of TiO₂ had a great influence on both the morphology and the sensing property of TiO₂-PANI/PA6 composite nanofibers.

Keywords: electrospinning; sputtering; nanofiber; sensor

1. Introduction

Ammonia is a toxic gas with very penetrating odor. High concentrations of ammonia constitute a threat to human health. Exposure to high ammonia concentrations of 1,000 ppm or more can cause pulmonary edema and accumulation of fluid in the lungs, leading to difficulty with breathing and

tightness in the chest. Today, most of the ammonia in our atmosphere is emitted directly or indirectly by human activity. The majority of all man-made ammonia is used for the production of fertilizers and for use in refrigeration systems [1]. Because the chemical industry, fertilizer factories and refrigeration systems make use of almost pure ammonia, a leak in the system, especially in ammonia production plants where ammonia is produced, can result in life-threatening situations.

Conducting polymers such as polypyrrole, polyaniline, polythiophene and their derivatives are being explored as promising materials for microsensors, because of their good ability to form chemical sensors either as a sensing element or as matrices to immobilize specific reagents. Among these conducting polymers, polyaniline nanomaterials are the most extensively studied because of their greater surface area that allows fast diffusion of gas molecules into the structure [2], and they have been successfully demonstrated as efficient gas sensors for monitoring airborne organic and inorganic components such as alcohol vapor [3,4], methanol [5], hydrogen [6,7], aromatic organic compounds (AOCs) [8], chloroform vapor [9,10], NO₂ [11], and especially ammonia [12–18]. Three major kinds of PANI-based ammonia sensing composite materials are described in the literature, including PANI-polymer composite [19,20], PANI-CNTs (or PANI-MWCNTs) composite [21,22] and PANI-metal dioxide composites (such as PANI-SnO₂ [23], PANI-In₂O₃ [23], PANI-ZnO [24] and PANI-TiO₂ [25,26]). Recently, more attention has been given to composite materials of PANI and metal dioxide, and ammonia sensing composites based on PANI and TiO₂.

In this work, PA6 nanofibers obtained by an electrospinning technique were first used as template to fabricate PANI/PA6 composite nanofibers by *in situ* polymerization. Then, TiO₂-PANI/PA6 composite nanofibers were prepared by depositing TiO₂ onto the PANI/PA6 substrate via RF magnetron sputtering. The TiO₂-PANI/PA6 composite nanofibers were finally fabricated into sensing devices for sensing application.

2. Experimental Section

2.1. Materials

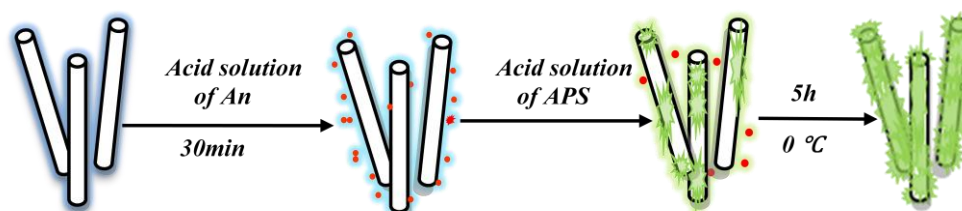
Aniline, formic acid (FA), ammonium persulfate (APS), ammonia and sulfuric acid (H₂SO₄) were purchased from Sinopharm Chemical Reagent Co. Ltd. (Beijing, China). Polyamide 6 (PA6, Mw = 21,000 g/mol) was obtained from ZIG ZHENG Industrial Co. Ltd (Taibei, Taiwan). All chemicals and reagents were used as received, except for aniline, which was distilled before use.

2.2. Fabrication of PANI/PA6 Composite Nanofibers

PANI/PA6 composite nanofibers were prepared by electrospinning and *in situ* polymerization. PA6 nanofibers were firstly prepared by electrospinning PA6/FA solutions of 20% PA6 concentration. Then, aniline and APS were dissolved separately in aqueous solutions, and the H⁺ concentrations of the aqueous solutions were adjusted by H₂SO₄ to 1.5 mol/L. The mole ratio of aniline to APS was 1:1. The electrospun PA6 nanofibers, were then immersed into the aniline/H₂SO₄ solution for 30 min. Successive polymerization was finally initiated by dropping the acid aqueous solution of APS into the above diffusion bath. PANI was synthesized on the surface of PA6 nanofibers and doped with H₂SO₄ at 0–5 °C for 5 h. After the reaction, the samples were taken out, washed with deionized water, and

dried in vacuum at 65 °C for 12 h. The steps for synthesis of PANI/PA6 composite nanofibers are illustrated in Figure 1.

Figure 1. Fabrication of PANI/PA6 composite nanofibers.



2.3. Fabrication of TiO₂-PANI/PA6 Composite Nanofibers

TiO₂-PANI/PA6 composite nanofibers were obtained by depositing TiO₂ onto PANI/PA6 substrate at room temperature for different times via RF magnetron sputtering. High purity titanium discs (99.99%) of 50 mm diameter was used as sputtering targets. High purity argon (99.999%) and oxygen (99.999%) were used as the sputtering and reactive gases, respectively. A diffusion pump was used to get the desired 9.8×10^{-4} Pa base pressure. The argon and oxygen flow rates were controlled separately by mass flow meters. The distance between target and substrates was kept at 60 mm. Before each sputtering-deposition step, the target was pre-sputtered in argon for 10 min to clean the target surface. The sputtering conditions are listed in Table 1.

Table 1. Sputtering conditions.

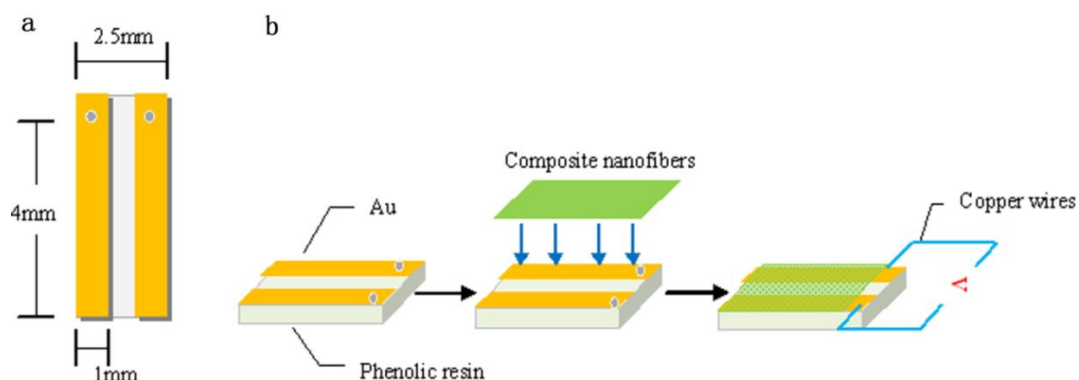
Deposition time (min)	Sputtering power (W)	Total pressure (Pa)	Oxygen and argon flow rates (mL/min)/(mL/min)
30	80	0.5	10/80
60			
90			

2.4. Characterization

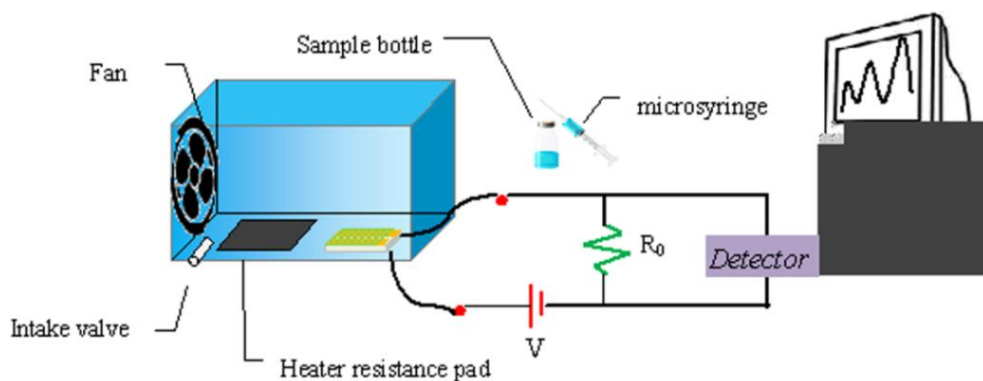
The structure and surface morphology of PANI/PA6 and TiO₂-PANI/PA6 composite nanofibers were observed with a field emission scanning electron microscope (FESEM, S-4800, Hitachi, Tokyo, Japan) with a golden coating. Fourier transform infrared (FTIR) spectrum of all the samples was obtained with a resolution of 4 cm⁻¹ in the range of 400–4,000 cm⁻¹ by using a NEXUS 470 spectrometer (Nicolet, Madison, WI, USA).

2.5. Gas Sensing Test

A sensing system for ammonia sensing test was fabricated by the following processes. A home-made Au electrode with a gap of 0.5 mm between two Au stripes was firstly prepared by depositing Au on phenolic resin, and then PANI/PA6 and TiO₂-PANI/PA6 composite nanofibers were pasted onto the open area between the two electrodes as shown in Figure 2.

Figure 2. Schematic illustration of (a) home-made Au electrode and (b) sensing electrode.

To test the ammonia sensitivity, the sensing electrode was placed in a lab-made sensing system as shown in Figure 3. The sensing set-up consisted of an airtight test chamber with 4,500 mL volume, a heater pad and a fan. Two minutes after the system reached a steady-state, a certain amount of ammonia was injected with a microsyringe through the intake valve, and with the help of a heater pad, the ammonia was heated to evaporation. The resistance changes of PANI/PA6 and TiO₂-PANI/PA6 composite nanofibers sensors were monitored and recorded automatically by an Agilent electrometer and a computer. A constant voltage of 5.0 V was used as the DC power supply. All the tests were conducted at room temperature (25 ± 1 °C) with a relative humidity of $65 \pm 1\%$.

Figure 3. Schematic illustration of lab-made sensing system.

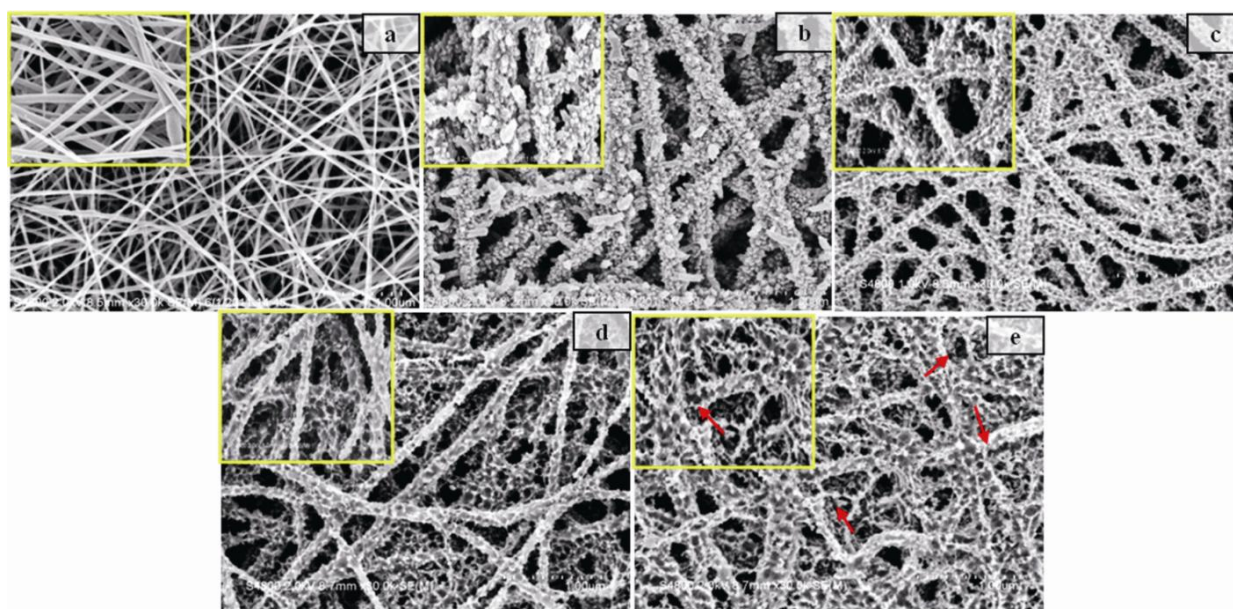
During the measurements, the actual ammonia volumes injected were 0.67, 1.35, 2.02, 2.69 and 3.37 μL , corresponding to the ammonia vapor with the concentration of 50, 100, 150, 200 and 250 ppm, respectively. After the ammonia was introduced to the chamber, the resistance of the sensors was recorded for 250 s, then the test chamber was flushed with dry air consecutively for another 250 s to make sure that a relatively steady state had achieved before next cyclic test. The sensitivity is defined as $(R_i - R_0)/R_0$, where R_i and R_0 are the resistance of sensors in ammonia and in air, respectively. The response and recovery time are defined as the time of 90% total resistance change. Each result was the average value of fivetimed tests.

3. Results and Discussion

3.1. Surface Morphology

It is well known that structure and morphology can have a significant effect on the sensing properties of materials. The SEM images of PA6 nanofibers, PANI/PA6 composite nanofibers and TiO₂-PANI/PA6 composite nanofibers sputtered for different times are shown in Figure 4. It can be seen that the surface morphology of PA6 nanofibers appeared smooth, while PANI/PA6 composite nanofibers had a rough surface and more uniform diameter because of the PANI coating, as indicated in Figure 4(a,b). The SEM images clearly revealed that the TiO₂-PANI/PA6 composite nanofibers had very rough surface with porous structures, as presented in Figure 4(c–e). This could be attributed to the impact of high-energy particles during sputtering deposition of TiO₂. It is obvious that such porous structure exhibited higher specific surface area than PANI/PA6, which facilitated the diffusion of ammonia vapor in sensing materials. However, TiO₂-PANI/PA6 with 90 min deposition time showed a distorted surface structure as the excessive sputtering time could damage the integrity of the PANI coating.

Figure 4. SEM image of (a) PA6 nanofibers; (b) PANI/PA6 nanofibers; (c) PANI/PA6 nanofibers sputtered for 30 min; (d) TiO₂-PANI/PA6 nanofibers sputtered for 60 min, (e) TiO₂-PANI/PA6 nanofibers sputtered for 90 min.

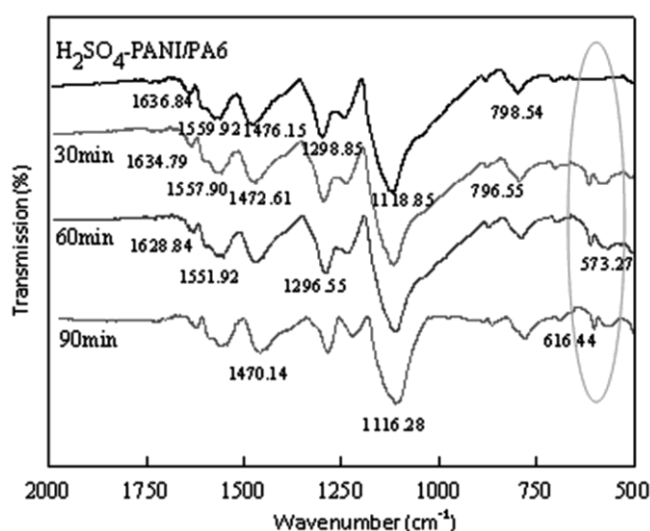


3.2. FTIR Analysis

The FTIR spectra of PANI/PA6 and TiO₂-PANI/PA6 composite nanofibers are shown in Figure 5. For the PANI/PA6 composite nanofibers, the peaks around 1,476.15 cm⁻¹ and 1,559.92 cm⁻¹ were assigned to C=C stretching vibrations of the benzenoid and quinoid rings, respectively. The peaks at 1,298.85 cm⁻¹ and 798.54 cm⁻¹ resulted from the C–N stretching vibration of the secondary aromatic amine and the C–H bending vibration, respectively. The characteristic peak of Q=NH⁺–B was also observed at around 1,118.85 cm⁻¹. All these peaks were identical to those of PANI. On the other hand,

the C=O stretching vibration peak of amide in PA6 was also observed at $1,636.84\text{ cm}^{-1}$, while the amide N–H stretching vibration peak overlapped with the C=C stretching peak of the PANI quinoid rings, thus the peak at $1,559.92\text{ cm}^{-1}$ was shown to be broader. All the characteristic peaks of PANI/PA6 could be observed in the spectrum of TiO_2 -PANI/PA6 composite nanofibers, and the characteristic bands around 616.44 cm^{-1} and 573.27 cm^{-1} was attributed to Ti–O bending vibration of TiO_2 . It also can be observed that incorporation of TiO_2 nanoparticles leads peaks of PANI/PA6 to shift slightly to lower wave number, indicating that some interaction existed between PANI and TiO_2 .

Figure 5. FTIR spectra of PANI/PA6 and TiO_2 -PANI/PA6 sputtered for 30 min, 60 min and 90 min, respectively.



3.3. Gas Response Behavior of Sensors

3.3.1. Effect of Sputtering Time

To investigate the effect of TiO_2 nanoparticles on the ammonia sensing properties, ammonia sensing comparison tests were carried out with PANI/PA6 and TiO_2 -PANI/PA6 sputtered for 30, 60 and 90 min. Figure 6 shows the dynamic response-recovery of all samples to 50, 100, 150, 200 and 250 ppm ammonia vapor. It can be seen that resistance of all samples increased dramatically when exposed to ammonia vapor and decreased gradually when dry air was introduced. Compared to PANI/PA6 nanofibers, all TiO_2 -PANI/PA6 composite nanofibers showed better ammonia sensitivity, as revealed in Figure 7. It is obvious that the sensitivity of ammonia sensing material improved greatly after TiO_2 deposition. It is also found that TiO_2 -PANI/PA6 sputtered for 60 min performed best among the samples prepared. Taking 250 ppm ammonia vapor for instance, the sensitivity of PANI/PA6 composite nanofibers was only 1.4, but the sensitivity of TiO_2 -PANI/PA6 composite nanofibers sputtered for 30 min increased to 5.2, and the sensitivity of TiO_2 -PANI/PA6 sputtered for 60 min was as high as 18.3. However, when the sputtering time was extended to 90 min, the sensitivity of TiO_2 -PANI/PA6 composite nanofibers was 15.1 with a small decline.

TiO_2 nanoparticles were deposited randomly on the PANI/PA6 substrate, which contributed to the good contact between TiO_2 and PANI. Sensing properties of PANI/PA6 were due to the reversible

chemisorptions of PANI [27,28], while the ammonia sensing behavior of TiO₂-PANI/PA6 composite nanofibers was the joint function of PANI and P-N junction formed between p-type PANI and n-type TiO₂. When exposed to the ammonia vapor, PANI was deprotonated by ammonia, which would increase the resistance of PANI and broaden the depletion layer thickness of P-N junction, as shown in Figure 8. The change of depletion layer thickness would increase the resistance of P-N junction. Therefore, the resistance changes in both PANI and P-N junction play a key role in controlling the current through the P-N composite sensor. In addition, because the absorption of ammonia would not only change the conductivity of PANI particles but also the resistance of P-N junction, the increase of TiO₂ content in the nanofibers could result in an increase in the sensitivity of the nanofiber sensors at low ranges of TiO₂ content. However, too high a content of TiO₂ resulting from overlong sputtering times would damage the continuous phase of PANI layer, as revealed in Figure 4(e).

Figure 6. Dynamic response and recovery of (a) PANI/PA6; (b) TiO₂-PANI/PA6 sputtered for 30 min; (c) TiO₂-PANI/PA6 sputtered for 60 min and (d) TiO₂-PANI/PA6 sputtered for 90 min to ammonia vapor of different concentrations.

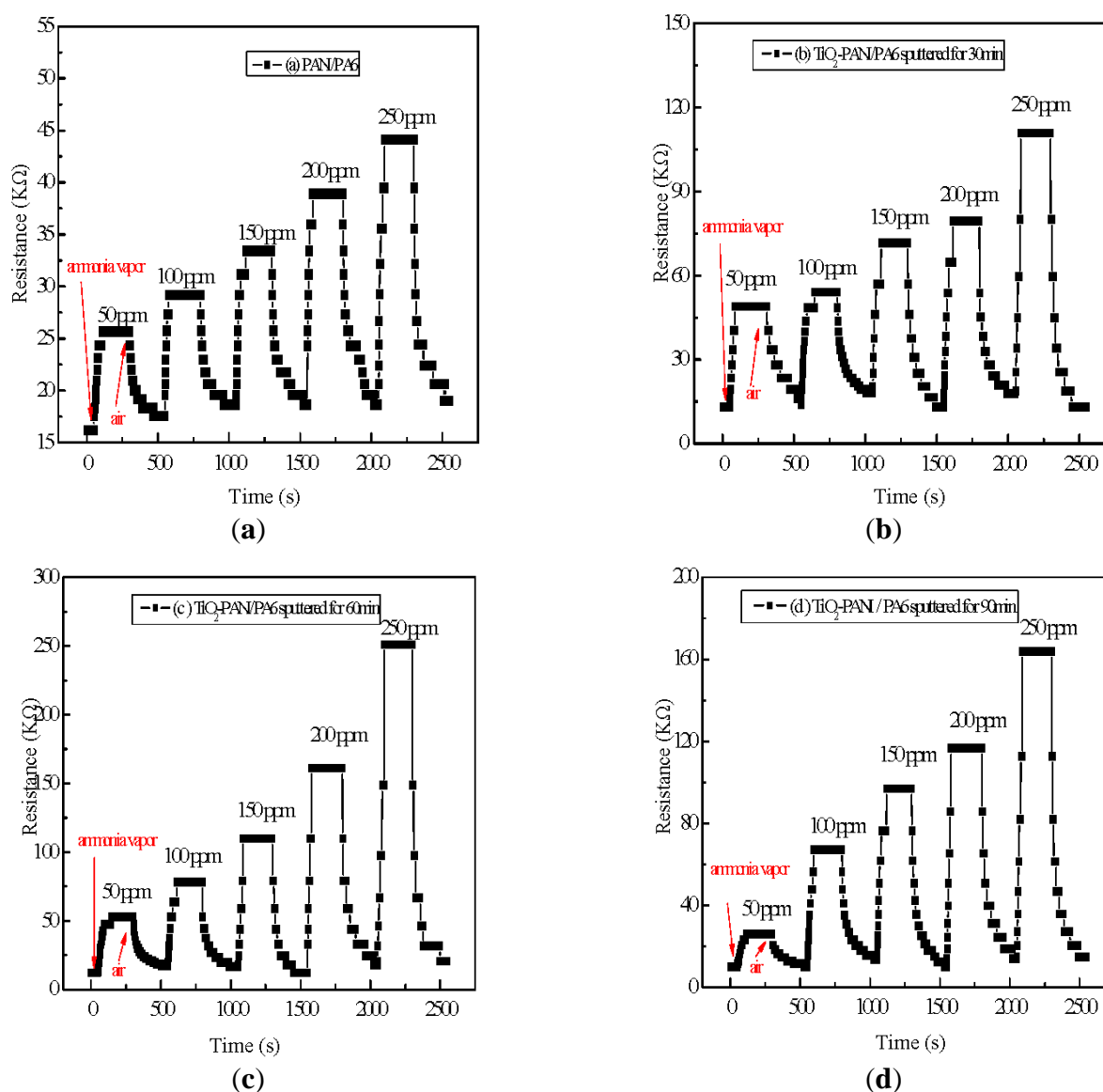


Figure 7. Sensitivity of (a) PANI/PA6; (b) TiO₂-PANI/PA6 sputtered for 30 min; (c) TiO₂-PANI/PA6 sputtered for 60 min and (d) TiO₂-PANI/PA6 sputtered for 90 min to ammonia vapor of different concentrations.

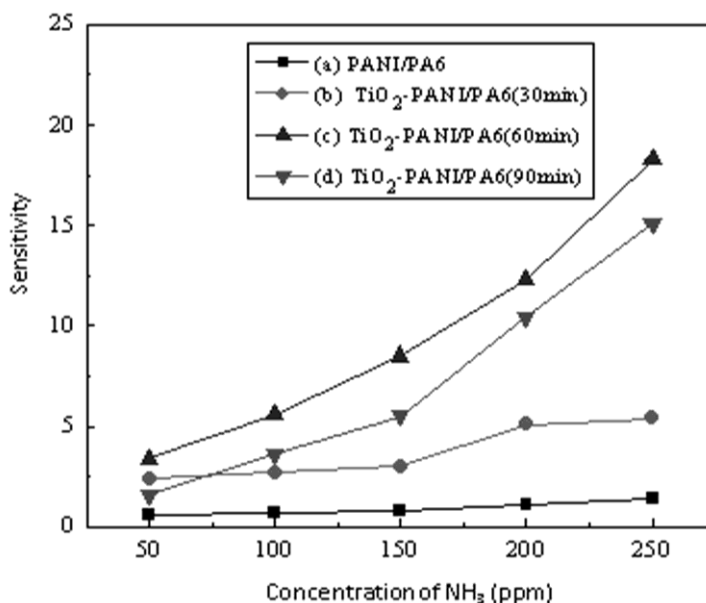
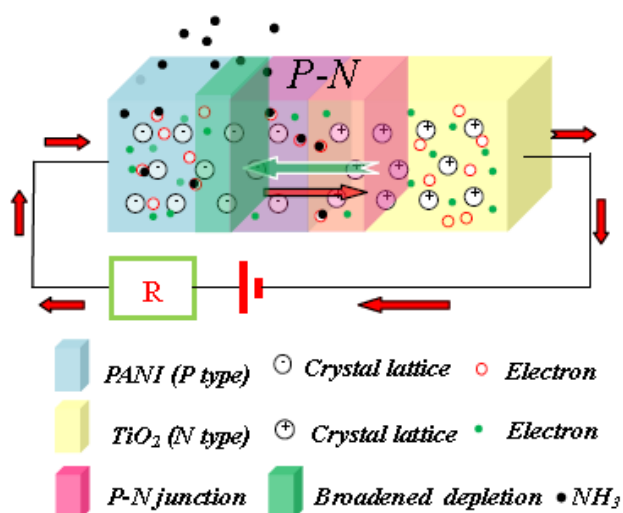
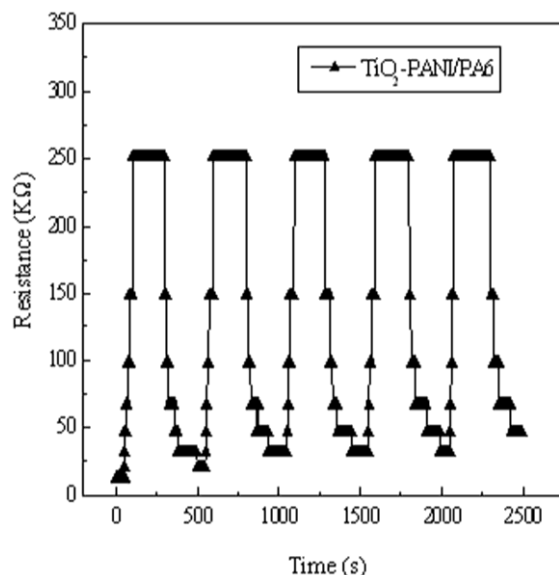


Figure 8. The effect of NH₃ on the depletion layer of TiO₂-PANI P-N junction.



3.3.2. Sensing Cyclability of Composite Nanofibers

The reliability of sensing materials also depends on their repeated use. Figure 9 depicts the response of TiO₂-PANI/PA6 composite nanofibers sputtered for 60 min to successive exposures to 250 ppm ammonia vapor. The resistance remained constant after repeat uses, indicating the good reproducibility of the material.

Figure 9. Cyclability of TiO₂-PANI/PA6 to ammonia vapor of 250 ppm.

4. Conclusions

From the above mentioned studies, it has been concluded that TiO₂-PANI/PA6 composite nanofibers were successfully fabricated via the combination of *in situ* chemical polymerization and sputtering, which was a new, easy-to-handle and inexpensive technique. P-N junctions formed between PANI and TiO₂ played a key role in the sensing behavior of TiO₂-PANI/PA6 composite nanofibers to ammonia, which lead to a better sensitivity to ammonia such as higher response sensitivity, better response and recovery, compared to PANI/PA6 composite nanofibers. It clearly appeared that the content of TiO₂ component controlled by sputtering-deposition time influenced the morphology and sensing property of TiO₂-PANI/PA6 composite nanofibers. The gas-sensing properties of TiO₂-PANI/PA6 composite nanofibers to ammonia, methanol, and ethanol and acetone vapor indicated that TiO₂-PANI/PA6 composite nanofibers had excellent selectivity for ammonia detection, but would not applicable for the fabrication of methanol, ethanol and acetone vapor sensors. Further work will be devoted to improving the stability of the TiO₂-PANI/PA6 composite nanofibers sensor.

Acknowledgments

This work was financially supported by the National High-tech R&D Program of China (No. 2012AA030313), Changjiang Scholars and Innovative Research Team in University (No. IRT1135), National Natural Science Foundation of China (No. 51006046 and No. 51163014), the Priority Academic Program Development of Jiangsu Higher Education Institutions, and the Research Fund for Doctoral Program of Higher Education of China (No. 20090093110004).

References

1. Timmer, B.; Olthuis, W.; van den Berg, Albert. Ammonia sensors and their applications—A review. *Sens. Actuators B Chem.* **2005**, *107*, 666–677.
2. Rajesh, T.A.; Kumar, D. Recent progress in the development of nano-structured conducting polymers/nanocomposites for sensor applications. *Sens. Actuators B Chem.* **2009**, *136*, 275–286.
3. Mohamad, M.A.; Gad, E.H.; Nagy, L.T. A sensor of alcohol vapor based on thin polyaniline base film and quartz crystal microbalance. *J. Hazard. Mater.* **2009**, *168*, 85–88.
4. Mohamad, M.A.; Nagy, L.T. Alcohol vapors sensor based on thin polyaniline salt film and quartz crystal microbalance. *Talanta* **2009**, *78*, 1280–1285.
5. Athawale, A.A.; Bhagwat, S.V.; Katre, P.P. Nanocomposite of Pd-polyaniline as a selective methanol sensor. *Sens. Actuators B Chem.* **2006**, *114*, 263–267.
6. Sadek, A.Z.; Wlodarski, W.; Zadeh, K.K.; Baker, C.; Kaner, R.B. Doped and dedoped polyaniline nanofibers based conductometric hydrogen gas sensors. *Sens. Actuators A Phys.* **2007**, *139*, 53–57.
7. Arsat, R.; Yu, X.F.; Li, Y.X.; Wlodarski, W.; Kalantar-zadeh, K. Hydrogen gas sensor based on highly ordered polyaniline nanofibers. *Sens. Actuators B Chem.* **2009**, *137*, 529–532.
8. Li, W.; Hoa, N.D.; Cho, Y.; Kim, D.; Kim, J.S. Nanofibers of conducting polyaniline for aromatic organic compound sensor. *Sens. Actuators B Chem.* **2009**, *143*, 132–138.
9. Li, Z.F.; Blum, F.D.; Bertino, M.F.; Kim, C.S.; Pillalamarri, S.K. One-step fabrication of a polyaniline nanofibers vapor sensor. *Sens. Actuators B Chem.* **2008**, *134*, 31–35.

10. Sharma, S.; Nirkhe, C.; Pethkar, S.; Athawale, A.A. Chloroform vapour sensor based on copper/polyaniline nanocomposite. *Sens. Actuators B Chem.* **2002**, *85*, 131–136.
11. Kumar, R.; Singh, S.; Misra, A.K. Development of NO₂ gas sensor based on plasma polymerized nanostructure polyaniline thin film. *J. Miner. Mater. Charact. Eng.* **2010**, *9*, 997–1006.
12. Masanobu, M.; Takuya, A. Properties and stability of polyaniline nanofibers ammonia sensors fabricated by novel on-substrate method. *Sens. Actuators B Chem.* **2011**, *160*, 999–1004.
13. Stamenov, P.; Madathil, R.; Coey, J.M.D. Dynamic response of ammonia sensors constructed from polyaniline nanofibre films with varying morphology. *Sens. Actuators B Chem.* **2012**, *163*, 989–999.
14. Sutar, D.S.; Padma, N.; Aswal, D.K.; Deshpande, S.K.; Gupta, S.K.; Yakhmi, J.V. Preparation of nanofibrous polyaniline films and their application as ammonia gas sensor. *Sens. Actuators B Chem.* **2007**, *128*, 286–292.
15. Manigandan, S.; Jain, A.; Majumder, S.; Ganguly, S.; Kargupta, K. Formation of nanorods and nanoparticles of polyaniline using Langmuir Blodgett technique: Performance study of ammonia sensor. *Sens. Actuators B Chem.* **2008**, *133*, 187–194.
16. Crowley, K.; Morrin, A.; Hernandez, A.; Malley, E.O.; Whitten, G.P. Fabrication of an ammonia gas sensor using inkjet-printed polyaniline nanoparticles. *Talanta* **2008**, *77*, 710–717.
17. Xing, S.X.; Zhao, C.; Jing, S.Y.; Wu, Y.; Wang, Z.C. Morphology and gas-sensing behavior of *in situ* polymerized nanostructured polyaniline films. *Eur. Polym. J.* **2006**, *42*, 2730–2735.
18. Tuan, C.V.; Tuan, M.A.; Hieu, N.V.; Trung, T. Electrochemical synthesis of polyaniline nanowires on printer digitated microelectrode for room temperature NH₃ gas sensor application. *Appl. Phys.* **2012**, *12*, 1011–1016.
19. Singh, V.; Mohan, S.; Singh, G.; Pandey, P.C.; Prakash, R. Synthesis and characterization of polyaniline-carboxylated PVC composites: Application in development of ammonia sensor. *Sens. Actuators B Chem.* **2008**, *132*, 99–106.
20. Nicho, M.E.; Trejo, M.; Valenzuela, A.G.; Saniger, J.M.; Palacios, J.; Hu, H. Polyaniline composite coatings interrogated by nulling optical-transmittance bridge for sensing low concentrations of ammonia gas. *Sens. Actuators B Chem.* **2001**, *76*, 18–24.
21. Yun, J.M.; Im, J.S.; Kim, H.-I.; Lee, Y.S. Effect of oxyfluorination on gas sensing behavior of polyaniline-coated multi-walled carbon nanotubes. *Appl. Surf. Sci.* **2012**, *258*, 3462–3468.
22. Yoo, K.P.; Kwon, K.H.; Min, N.K.; Lee, M.J.; Lee, C.J. Effects of O₂ plasma treatment on NH₃ sensing characteristics of multiwall carbon nanotube/polyaniline composite films. *Sens. Actuators B Chem.* **2009**, *143*, 333–340.
23. Tai, H.L.; Jiang, Y.D.; Xie, G.Z.; Yu, J.S. Preparation, characterization and comparative NH₃-sensing characteristic studies of PANI/inorganic oxides nanocomposite thin films. *J. Mater. Sci. Technol.* **2010**, *26*, 605–613.
24. Patil, L.; Chougule, M.A.; Sen, S.; Patil, V.B. Measurements on room temperature gas sensing properties of CSA doped polyaniline-ZnO nanocomposites. *Meas. Sci. Technol.* **2012**, *45*, 243–249.
25. Gong, J.; Li, Y.H.; Hu, Z.S.; Zhou, Z.Z.; Deng, Y.L. Ultrasensitive NH₃ gas sensor from polyaniline nanograin enshased TiO₂ fibers. *J. Phys. Chem. C* **2010**, *114*, 9970–9974.

26. Li, Y.H.; Gong, J.; He, G.H.; Deng, Y.L. Fabrication of polyaniline/titanium dioxide composite nanofibers for gas sensing application. *Mater. Chem. Phys.* **2011**, *129*, 477–482.
27. Sengupta, P.P.; Kar, P.; Adhikari, B. Influence of dopant in the synthesis, characteristics and ammonia sensing behavior of processable polyaniline. *Thin Solid Films* **2009**, *517*, 3770–3775.
28. Hu, H.; Trejo, M.; Nicho, M.E.; Saniger, J.M.; Garcia-Valenzuela, A. Adsorption kinetics of optochemical NH₃ gas sensing with semiconductor polyaniline films. *Sens. Actuators B Chem.* **2002**, *82*, 14–23.

© 2012 by the authors; licensee MDPI, Basel, Switzerland. This article is an open access article distributed under the terms and conditions of the Creative Commons Attribution license (<http://creativecommons.org/licenses/by/3.0/>).